# Synthesis and Characterization of the Polyoxoanion-Supported $Ru^I$–$Ru^I$ Tetracarbonyls $[(P_3O_9)_2Ru_2(CO)_4]^{4-}$ and $[(Cp^*TiW_5O_{18})_2Ru_2(CO)_4]^{4-}$

**Walter G. Klemperer* and Bianxiao Zhong**

Department of Chemistry, University of Illinois, Urbana, Illinois 61801

*Received July 14, 1993*®

Five new $Ru^I$–$Ru^I$ tetracarbonyl complexes, including two incorporating polyoxoanion ligands, have been prepared: $[(P_3O_9)_2Ru_2(CO)_4]^{4-}$ (**1**), $[(Cp^*TiW_5O_{18})_2Ru_2(CO)_4]^{4-}$ (**2**), $[(CH_3CN)_6Ru_2(CO)_4]^{2+}$ (**3**), $[(PPh_3)_2(CH_3CN)_4Ru_2(CO)_4]^{2+}$ (**4**), and $[(C_5H_5N)_6Ru_2(CO)_4]^{2+}$ (**5**). Two of these complexes were structurally characterized in the solid state using single-crystal X-ray diffraction techniques: complex **1** as a solvated tetra-*n*-butylammonium salt $[[(P_3O_9)_2Ru_2(CO)_4](TBA)_4{\cdot}2CH_3CN$: $a = 11.737(1)$ Å, $b = 16.166(3)$ Å, $c = 24.583(7)$ Å, $\beta = 100.19(2)°$, $Z = 2$, space group $P2_1/c\text{-}C_{2h}^5$] and complex **4** as a hexafluorophosphate salt $[[(PPh_3)_2(CH_3CN)_4Ru_2(CO)_4](PF_6)_2$: $a = 29.157(5)$ Å, $b = 9.341(2)$ Å, $c = 20.673(3)$ Å, $\beta = 108.40(5)°$, $Z = 4$, space group $C2/c\text{-}C_{2h}^6$]. The remaining were formulated and assigned structures on the basis of their elemental compositions, NMR spectra, and infrared spectra. Complex **3** proved to be a reactive precursor to a variety of $Ru^I$–$Ru^I$ tetracarbonyl complexes, including complexes **1**, **2**, **4**, and **5**.

## Introduction

As part of a continuing effort to prepare polyoxoanion-supported organoruthenium complexes that are reactive toward oxygen under mild conditions,[1] we have targeted metal–metal-bonded $Ru^I$ species with the hope that these species, like the metal-metal bonded $Mo^I$ dimer $[(C_5Me_5)Mo(CO)_3]_2$, might yield oxo complexes upon oxidation.[2] Specifically, polyoxoanion analogues of the cyclopentadienyl complexes $[CpRu(CO)_2]_2$, Cp = $C_5H_5$,[3] $C_5Me_4Et$,[4] and $C_5Me_5$,[5] have served as synthetic objectives, where the $Cp^-$ ligand is replaced by the tridentate ligands $P_3O_9^{3-}$ [1,6] and $Cp^*TiW_5O_{18}^{3-}$,[1,7] $Cp^* = C_5(CH_3)_5$. The synthesis and characterization of these two complexes, $[(P_3O_9)_2Ru_2(CO)_4]^{4-}$ and $[(Cp^*TiW_5O_{18})_2Ru_2(CO)_4]^{4-}$, are the focus of the studies reported here. The synthesis and substitution chemistry of a reactive precursor to these complexes, $[(CH_3CN)_6Ru_2(CO)_4]^{2+}$, are also described.

## Results and Discussion

Results of the synthetic studies reported below are summarized in Scheme I. The halide-bridged $Ru^{II}$ dimer $[Ru(CO)_3Cl_2]_2$,[8] while sufficiently reactive to form $[(P_3O_9)_2Ru_2(CO)_4]^{4-}$ (**1**) upon reaction with $P_3O_9^{3-}$, failed to form the analogous $Cp^*TiW_5O_{18}^{3-}$ derivative, **2**. Since acetonitrile complexes such as $[(OC)_3M(NCCH_3)_3]^+$ (M = Mn, Re), $[Cp^*Rh(NCCH_3)_3]^{2+}$, $[(C_7H_8)Rh(NCCH_3)_2]^+$, $[(C_8H_{12})Ir(NCCH_3)_2]^+$, $[(C_8H_{12})Ru(NCCH_3)_4]^{2+}$, and $(C_6H_6)Ru(NCCH_3)_3]^{2+}$ are known to be reactive toward polyoxoanion ligands,[9] the $Ru^I$–$Ru^I$ tetracarbonyl analogue $[(CH_3CN)_6Ru_2(CO)_4]^{2+}$ (**3**) was prepared and structurally characterized along with its triphenylphosphine derivative, **4**. Complex **3** proved to be a suitable precursor for complex **2**

**Scheme I**

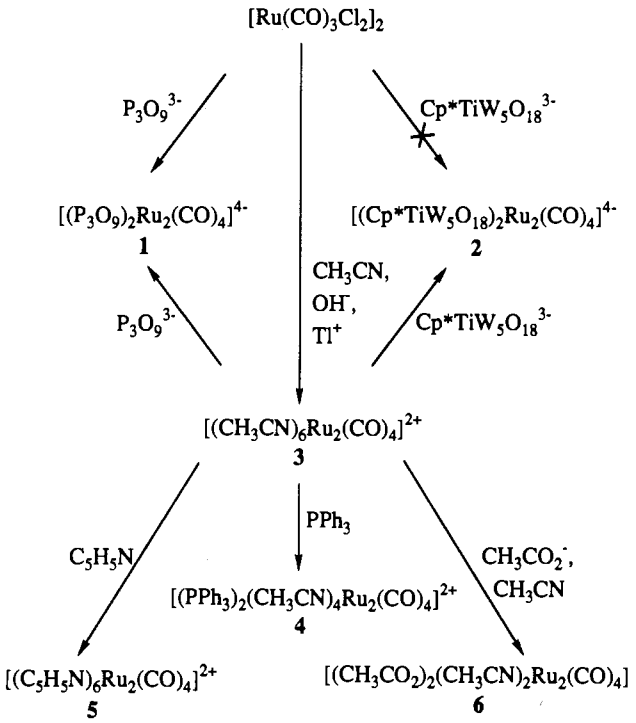


* Abstract published in *Advance ACS Abstracts,* November 1, 1993.

(1) Day, V. W.; Eberspacher, T. A.; Klemperer, W. G.; Planalp, R. P.; Schiller, P. W.; Yagasaki, A.; Zhong, B. *Inorg. Chem.* **1993**, *32*, 1629.
(2) Faller, J. W.; Ma, Y. *J. Organomet. Chem.* **1988**, *340*, 59.
(3) Mills, O. S.; Nice, J. P. *J. Organomet. Chem.* **1967**, *9*, 339.
(4) Bailey, N. A.; Radford, S. L.; Sanderson, J. A.; Tabatabaian, K.; White, C.; Worthington, J. M. *J. Organomet. Chem.* **1978**, *154*, 343.
(5) Steiner, A.; Gornitzka, H.; Stalke, D.; Edelmann F. T. *J. Organomet. Chem.* **1992**, *431*, C21.
(6) (a) Besecker, C. J.; Klemperer, W. G. *J. Organomet. Chem.* **1981**, *205*, C31. (b) Besecker, C. J.; Day, V. W.; Klemperer, W. G. *Organometallics* **1985**, *3*, 564. (c) Day, V. W.; Klemperer, W. G.; Schwartz, C.; Wang, R.-C. In *Surface Organometallic Chemistry: Molecular Approaches to Surface Catalysis*; Basset, J.-M., Gates, B. C., Candy, J.-P., Choplin, A., Leconte, M., Quignard, F., Santini, C., Eds.; Kluwer: Dordrecht, Holland, 1988; p 173. (d) Day, V. W.; Klemperer, W. G.; Lockledge, S. P.; Main, D. J.; Rosenberg, F. S.; Wang, R.-C.; Yaghi, O. M. In *Metal-Metal Bonds in Chemistry and Catalysis*; Fackler, J. P., Ed.; Plenum: New York, 1990; p 161. (e) Day, V. W.; Klemperer, W. G.; Main, D. J. *Inorg. Chem.* **1990**, *29*, 2345. (f) Klemperer, W. G.; Main, D. J. *Inorg. Chem.* **1990**, *29*, 2355. (g) Day, V. W.; Klemperer, W. G.; Lockledge, S. P.; Main, D. J. *J. Am. Chem. Soc.* **1990**, *112*, 2031. (h) Chen, J.; Day, V. W.; Eberspacher, T.; Klemperer, W. G. Submitted for publication.
(7) (a) Klemperer, W. G.; Yagasaki, A. *Chem. Lett.* **1989**, 2041. (b) Che, T. M.; Day, V. W.; Francesconi, L. C.; Klemperer, W. G.; Main, D. J.; Yagasaki, A.; Yaghi, O. M. *Inorg. Chem.* **1992**, *31*, 2920.
(8) Mantovani, A.; Cenini, S. *Inorg. Synth.* **1990**, *28*, 334 and references cited therein.
(9) (a) Besecker, C. J.; Klemperer, W. G. *J. Am. Chem. Soc.* **1980**, *102*, 7598. (b) Besecker, C. J.; Klemperer, W. G.; Day, V. W. *J. Am. Chem. Soc.* **1982**, *104*, 6158. (c) Besecker, C. J.; Day, V. W.; Klemperer, W. G.; Thompson, M. R. *J. Am. Chem. Soc.* **1984**, *106*, 4125. (d) Besecker, C. J.; Day, V. W.; Klemperer, W. G.; Thompson, M. R. *Inorg. Chem.* **1985**, *24*, 44. (e) Reference 6b. (f) Reference 7a. (g) Reference 6e. (h) Reference 6f. (i) Reference 1.

0020-1669/93/1332-5821$04.00/0 

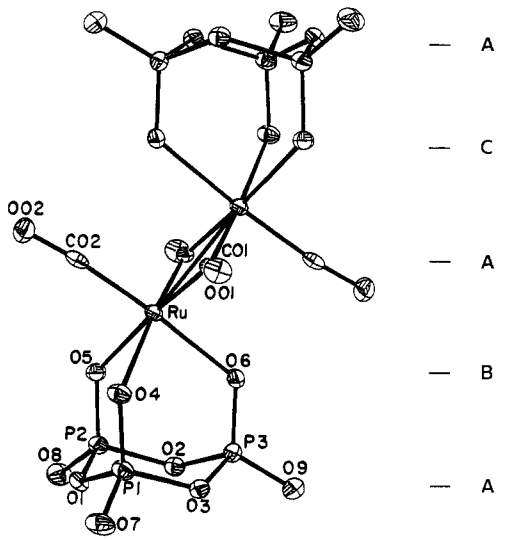


**Figure 1.** Perspective drawing of the $[(P_3O_9)_2Ru_2(CO)_4]^{4-}$ anion present in crystalline $[(P_3O_9)_2Ru_2(CO)_4](TBA)_4{\cdot}2CH_3CN$. Atoms are represented by thermal vibration ellipsoids drawn to encompass 35% of their electron density. The packing sequence of closest-packed oxygen and CO layers is indicated on the far right side of the figure.

**Table I.** Crystallographic Data for $[(P_3O_9)_2Ru_2(CO)_4][(n\text{-}C_4H_9)_4N]_4{\cdot}2CH_3CN$ (I) and $[(PPh_3)_2(CH_3CN)_4Ru_2(CO)_4](PF_6)_2$ (II)

| | I | II |
|---|---|---|
| formula | $Ru_2P_6O_{22}N_6C_{72}H_{150}$ | $Ru_2P_4F_{12}O_4N_4C_{48}H_{42}$ |
| fw | 1840.00 | 1292.90 |
| space group | $P2_1/c\text{-}C_{2h}^5$ | $C2/c\text{-}C_{2h}^6$ |
| $a$, Å | 11.737(1) | 29.157(5) |
| $b$, Å | 16.166(3) | 9.341(2) |
| $c$, Å | 24.583(7) | 20.673(3) |
| $\beta$, deg | 100.19(2) | 108.40(1) |
| $V$, Å$^3$ | 4591(3) | 5343(4) |
| $Z$ | 2 | 4 |
| $\rho_{calcd}$, g cm$^{-3}$ | 1.331 | 1.607 |
| $T$, °C | −75 ± 1 | 20 ± 1 |
| $\mu$, mm$^{-1}$ | 0.489 | 0.757 |
| transm coeff | 0.877–0.909 | 0.811–0.876 |
| radiation | Mo K$\alpha$ | Mo K$\alpha$ |
| $R(F_o)$[11] | 0.039 | 0.043 |
| $R_w(F_o)$[11] | 0.043 | 0.050 |

and complex **1** as well as other derivatives such as the pyridine complex $[(C_5H_5N)_6Ru_2(CO)_4]^{2+}$ (**5**) and the known[10] acetate complex $[(CH_3CO_2)_2(CH_3CN)_2Ru_2(CO)_4]$ (**6**).

**$[(P_3O_9)_2Ru_2(CO)_4]^{4-}$ (1).** Reaction of $[Ru(CO)_3Cl_2]_2$[8] with 4 equiv of $P_3O_9(TBA)_3{\cdot}2.5H_2O$, TBA = tetra-*n*-butylammonium,[6b] in acetonitrile followed by crystallization from $CH_2Cl_2/(C_2H_5)_2O$ yielded analytically pure $[(P_3O_9)_2Ru_2(CO)_4](TBA)_4{\cdot}2H_2O$ in 45% yield. Monitoring the reaction by $^{31}P$ NMR spectroscopy showed that 4 equiv of $P_3O_9^{3-}$ was necessary to optimize the reaction yield, suggesting the balanced equation (1).

$$[Ru(CO)_3Cl_2]_2 + 4P_3O_9^{3-} + H_2O = [(P_3O_9)_2Ru_2(CO)_4]^{4-} + 4Cl^- + 2HP_3O_9^{2-} + CO + CO_2 \quad (1)$$

A single-crystal X-ray diffraction study of $[(P_3O_9)_2Ru_2(CO)_4](TBA)_4{\cdot}2CH_3CN$ (see Table I), obtained by recrystallization of the dihydrate from $CH_3CN$/ether, revealed the presence of discrete dinuclear $[(P_3O_9)_2Ru_2(CO)_4]^{4-}$ anions (Figure 1 and Table II). $N(C_4H_9)_4^+$ cations (Figure S1a[12] and Table SI[12]), and $CH_3CN$ solvent molecules of crystallization (Figure S1b[12] and Table SI[12]). The $[(P_3O_9)_2Ru_2(CO)_4]^{4-}$ anion is seen to have the same structure observed for crystalline $[CpRu(CO)_2]_2$, Cp = $C_5H_5$,[3] $C_5Me_4Et$,[4] and $C_5Me_5$,[5] where $\eta^5$-Cp ligands have been replaced by $\kappa^3$-*O*-$P_3O_9^{3-}$ ligands. Bond lengths and angles for the $[(P_3O_9)_2Ru_2(CO)_4]^{4-}$ anion, given in Table III, show that the anion approximates $C_{2h}$ symmetry, although it rigorously possesses only $C_i$ crystallographic symmetry. The geometry of the $P_3O_9^{3-}$ ligand is similar to that of the same ligand in the $[(CH_3CN)_3Ru(P_3O_9)]^-$ and $[(C_8H_{12})Ru(NH_2NCMe_2)(P_3O_9)]^-$ anions.[1]

The infrared spectrum of $[(P_3O_9)_2Ru_2(CO)_4](TBA)_4{\cdot}2CH_3CN$ in a Nujol mull displays two absorptions in the carbonyl stretching region, corresponding to bridging (1764 cm$^{-1}$) and

**Table II.** Atomic Coordinates for Atoms in the Anion of Crystalline $[(P_3O_9)_2Ru_2(CO)_4][(n\text{-}C_4H_9)_4N]_4{\cdot}2CH_3CN$[a]

| atom type[b] | fractional coordinates | | |
|---|---|---|---|
| | $x$ | $y$ | $z$ |
| Ru | 0.02721(3) | 0.46422(2) | 0.45503(2) |
| P1 | −0.0592(1) | 0.42352(8) | 0.32269(5) |
| P2 | 0.0547(1) | 0.29096(8) | 0.38683(5) |
| P3 | −0.1740(1) | 0.33673(8) | 0.39787(5) |
| O1 | 0.0258(3) | 0.3442(2) | 0.3301(1) |
| O2 | −0.0747(3) | 0.2683(2) | 0.3955(1) |
| O3 | −0.1731(3) | 0.3838(2) | 0.3401(1) |
| O4 | −0.0090(3) | 0.4865(2) | 0.3649(1) |
| O5 | 0.1066(3) | 0.3485(2) | 0.4322(1) |
| O6 | −0.1307(3) | 0.3963(2) | 0.4435(1) |
| O7 | −0.0851(3) | 0.4464(2) | 0.2641(1) |
| O8 | 0.1166(3) | 0.2159(2) | 0.3760(1) |
| O9 | −0.2845(3) | 0.2956(2) | 0.3966(1) |
| O01 | −0.0944(3) | 0.6271(2) | 0.4389(1) |
| O02 | 0.2592(3) | 0.5439(2) | 0.4651(1) |
| C01 | −0.0536(4) | 0.5701(3) | 0.4662(2) |
| C02 | 0.1679(5) | 0.5160(3) | 0.4633(2) |

[a] The numbers in parentheses are the estimated standard deviations in the last significant digit. [b] Atoms are labeled in agreement with Figure 1.

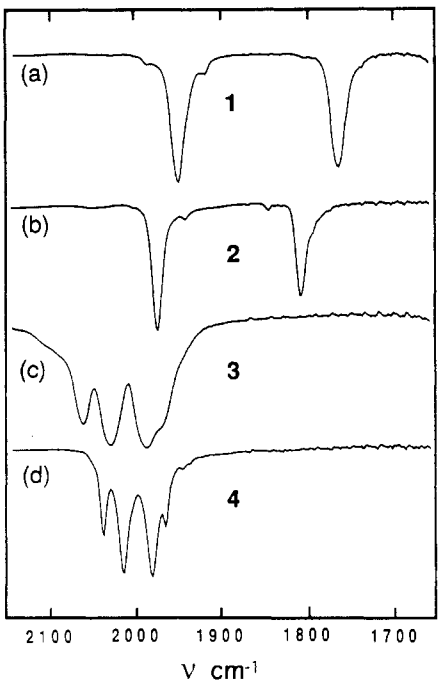


**Figure 2.** Infrared spectra recorded from Nujol mulls of (a) $[(P_3O_9)_2Ru_2(CO)_4](TBA)_4{\cdot}2H_2O$, (b) $[(Cp^*TiW_5O_{18})_2Ru_2(CO)_4](TBA)_4$, (c) $[(CH_3CN)_6Ru_2(CO)_4](PF_6)_2$, and (d) $[(PPh_3)_2(CH_3CN)_4Ru_2(CO)_4](PF_6)_2$. See Experimental Section for numerical data.

(10) (a) Crooks, G. R.; Johnson, B. F. G.; Lewis, J.; Williams, I. G. *J. Chem. Soc. A* **1969**, 2761. (b) Sherlock, S. J.; Cowie, M.; Singleton, E.; Steyn, M. M. d. V. *Organometallics* **1988**, *7*, 1663.

(11) The $R$ values are defined as $R = \sum||F_o| - |F_c||/\sum|F_o|$ and $R_w = [\sum w(|F_o| - |F_c|)^2/\sum w|F_o|^2]^{1/2}$, where $w = [\sigma(F)]^{-2}$ is the weight given each reflection. The function minimized is $\sum w(|F_o| - K|F_c|)^2$, where $K$ is the scale factor.

(12) See paragraph at end of paper regarding supplementary material.

**Table III.** Bond Lengths and Angles Involving Non-Hydrogen Atoms in the Anion of Crystalline $[(P_3O_9)_2Ru_2(CO)_4][(n\text{-}C_4H_9)_4N]_4\cdot 2CH_3CN$[a-c]

| | | | |
|---|---|---|---|
| | Bond Lengths (Å) | | |
| Ru–O4 | 2.211(3) | Ru–C01 | 1.998(5) |
| Ru–O5 | 2.207(3) | Ru–C01′ | 1.986(5) |
| Ru–O6 | 2.130(3) | Ru–C02 | 1.831(5) |
| P1–O4 | 1.498(3) | P1–O1 | 1.615(3) |
| P2–O5 | 1.497(3) | P1–O3 | 1.608(3) |
| P3–O6 | 1.497(3) | P2–O1 | 1.624(3) |
| P1–O7 | 1.465(3) | P2–O2 | 1.613(3) |
| P2–O8 | 1.464(4) | P3–O2 | 1.615(3) |
| P3–O9 | 1.453(4) | P3–O3 | 1.612(3) |
| O01–C01 | 1.190(6) | Ru–Ru′ | 2.6710(6) |
| O02–C02 | 1.155(6) | | |
| | Bond Angles (deg) | | |
| O4RuO5 | 84.2(2) | C01RuC01′ | 95.7(3) |
| O4RuO6 | 86.7(2) | C01RuC02 | 91.9(3) |
| O5RuO6 | 85.7(2) | C01′RuC02 | 92.1(3) |
| O4RuC01 | 89.2(2) | O4RuC02 | 92.7(2) |
| O5RuC01′ | 90.7(2) | O5RuC02 | 90.2(2) |
| O6RuC01 | 92.1(2) | O6RuC01′ | 88.2(2) |
| O4RuC01′ | 173.0(2) | O5RuC01 | 173.2(2) |
| O6RuC02 | 175.9(2) | | |
| RuO4P1 | 124.5(3) | P1O1P2 | 123.2(2) |
| RuO5P2 | 125.4(2) | P2O2P3 | 123.5(2) |
| RuO6P3 | 127.1(2) | P1O3P3 | 123.9(2) |
| O1P1O3 | 100.4(2) | O4P1O7 | 119.8(2) |
| O1P2O2 | 100.1(2) | O5P2O8 | 120.1(2) |
| O2P3O3 | 100.1(2) | O6P3O9 | 119.6(2) |
| O4P1O1 | 107.6(2) | O1P1O7 | 109.1(2) |
| O4P1O3 | 109.3(2) | O1P2O8 | 108.5(2) |
| O5P2O1 | 107.9(2) | O2P2O8 | 110.2(2) |
| O5P2O2 | 108.1(2) | O2P3O9 | 109.5(2) |
| O6P3O2 | 108.4(2) | O3P1O7 | 109.0(2) |
| O6P3O3 | 107.6(2) | O3P3O9 | 110.0(2) |
| RuC01Ru′ | 84.2(2) | RuC01O01 | 137.7(4) |
| RuC02O02 | 174.0(4) | | |

[a] The numbers in parentheses are the estimated standard deviations in the last significant digit. [b] Atoms are labeled in agreement with Figure 1. [c] Atoms labeled with primes are related to those labeled without primes by crystallographic inversion symmetry.

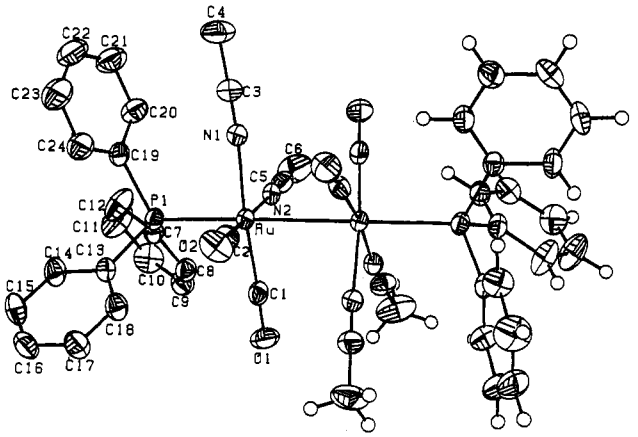


**Figure 3.** Perspective drawing of the $[(PPh_3)_2(CH_3CN)_4Ru_2(CO)_4]^{2+}$ cation present in crystalline $[(PPh_3)_2(CH_3CN)_4Ru_2(CO)_4](PF_6)_2$. All non-hydrogen atoms are represented by thermal vibration ellipsoids drawn to encompass 35% of their electron density; hydrogen atoms are represented by small spheres which are in no way representative of their true thermal motion.

terminal (1951 $cm^{-1}$) carbonyl groups (see Figure 2a). These stretching frequencies are in good agreement with the corresponding frequencies observed for $[(C_5H_5)Ru(CO)_2]_2$, namely, 1764 and 1946 $cm^{-1}$.[3] The $[(P_3O_9)_2Ru_2(CO)_4]^{2-}$ anion displays additional terminal carbonyl group absorptions in $CH_3CN$ and $CH_3NO_2$ solutions (see Experimental Section), presumably arising from isomers analogous to those observed for $[(C_5H_5)Ru(CO)_2]_2$ and $[(C_5H_5)Fe(CO)_2]_2$ in solution.[13]

**Table IV.** Atomic Coordinates for Selected Atoms in the Cation of Crystalline $[(PPh_3)_2(CH_3CN)_4Ru_2(CO)_4](PF_6)_2$[a]

| | fractional coordinates | | |
|---|---|---|---|
| atom type[b] | *x* | *y* | *z* |
| Ru | 0.44911(2) | 0.47616(5) | 0.21354(2) |
| P1 | 0.36309(5) | 0.4476(2) | 0.15325(8) |
| O1 | 0.4408(2) | 0.3741(6) | 0.3473(2) |
| O2 | 0.4475(2) | 0.7805(6) | 0.2590(3) |
| N1 | 0.4604(2) | 0.5563(6) | 0.1248(3) |
| N2 | 0.4585(2) | 0.2697(6) | 0.1787(3) |
| C1 | 0.4447(2) | 0.4104(7) | 0.2966(3) |
| C2 | 0.4476(2) | 0.6635(8) | 0.2427(3) |
| C3 | 0.4642(2) | 0.6053(8) | 0.0770(3) |
| C4 | 0.4672(3) | 0.6676(10) | 0.0138(4) |
| C5 | 0.4608(3) | 0.1579(8) | 0.1597(3) |
| C6 | 0.4627(4) | 0.0132(9) | 0.1356(4) |
| C7 | 0.3417(2) | 0.2609(7) | 0.1443(3) |
| C13 | 0.3206(2) | 0.5328(7) | 0.1892(3) |
| C19 | 0.3469(2) | 0.5181(8) | 0.0667(3) |

[a] The numbers in parentheses are the estimated standard deviations in the last significant digit. [b] Atoms are labeled in agreement with Figure 3.

**Table V.** Selected Bond Lengths and Angles for the Cation of Crystalline $[(PPh_3)_2(CH_3CN)_4Ru_2(CO)_4](PF_6)_2$[a-c]

| | | | |
|---|---|---|---|
| | Bond Lengths (Å) | | |
| Ru–C1 | 1.866(6) | Ru–N1 | 2.102(5) |
| Ru–C2 | 1.856(8) | Ru–N2 | 2.106(6) |
| Ru–P1 | 2.438(2) | Ru–Ru′ | 2.8731(8) |
| | Bond Angles (deg) | | |
| Ru′RuC1 | 82.9(2) | P1RuC1 | 94.3(2) |
| Ru′RuC2 | 87.5(2) | P1RuC2 | 98.2(2) |
| Ru′RuN1 | 92.1(1) | P1RuN1 | 90.7(1) |
| Ru′RuN2 | 87.4(1) | P1RuN2 | 87.1(1) |
| C1RuC2 | 89.8(3) | N1RuN2 | 87.4(2) |
| C1RuN2 | 93.8(2) | C2RuN1 | 88.5(2) |
| C1RuN1 | 174.9(2) | C2RuN2 | 173.4(2) |
| Ru′RuP1 | 173.69(4) | | |

[a] The numbers in parentheses are the estimated standard deviations in the last significant digit. [b] Atoms are labeled in agreement with Figure 3. [c] Ru′ is generated by 2-fold rotation symmetry from Ru.

**$[(CH_3CN)_6Ru_2(CO)_4]^{2+}$ (3) and $[(PPh_3)_2(CH_3CN)_4Ru_2(CO)_4]^{2+}$ (4).** Reaction of $[Ru(CO)_3Cl_2]_2$[8] suspended in $CH_3CN$ with 2 equiv of NaOH in EtOH followed by addition of 4 equiv of $TlPF_6$ yielded a solution from which analytically pure $[(CH_3CN)_6Ru_2(CO)_4](PF_6)_2$ could be isolated in 82% yield, implying the following balanced equation:

$$[Ru(CO)_3Cl_2]_2 + 2NaOH + 4TlPF_6 + 6CH_3CN = [(CH_3CN)_6Ru_2(CO)_4](PF_6)_2 + CO + CO_2 + H_2O + 2NaPF_6 + 4TlCl \quad (2)$$

The product is extremely substitution labile. When it is washed with diethyl ether and then dried in vacuo, its color changes from yellow to dark blue, but the yellow color is regenerated upon exposure of the solid to acetonitrile vapor. The blue solid is acetonitrile-deficient according to elemental analysis. Apparently, at least some of the acetonitrile ligands in anion **3** are replaced by diethyl ether, which is removed in vacuo to produce a blue complex. To avoid this dissociation in the preparation of $[(CH_3CN)_6Ru(CO)_4](PF_6)_2$, the final product is dissolved in acetonitrile and the solvent is then removed in vacuo. In this fashion, analytically pure material is obtained.

Since single crystals of $[(CH_3CN)_6Ru_2(CO)_4](PF_6)_2$ suitable for X-ray structural analysis could not be obtained, the triph-

(13) (a) Adams, R. D.; Cotton, F. A. In *Dynamic NMR Spectroscopy*; Jackman, L. M., Cotton, F. A., Eds.; Academic Press: New York, 1975; pp 503 and references cited therein. (b) Bennett, M. A.; Bruce, M. I. in *Comprehensive Organometallic Chemistry*; Wilkinson, G., Stone, F. G. A., Abel, E. W., Eds.; Pergamon: Oxford, U.K., 1982; Vol. 4, p 821, and references cited therein.

enylphosphine derivative $[(PPh_3)_2(CH_3CN)_4Ru_2(CO)_4]^{2+}$ (**4**) was prepared as a $PF_6^-$ salt from the $PF_6^-$ salt of **3** plus excess $PPh_3$. Single-crystal X-ray structural analysis of this material (see Table I) showed the presence of discrete, dinuclear, $C_2$-symmetric $[(PPh_3)_2(CH_3CN)_4Ru_2(CO)_4]^{2+}$ cations (Figure 3 and Table IV) and $PF_6^-$ anions (Table SIV[12]). Selected bond lengths and angles in the cation are given in Table V. Each ruthenium center in cation **4** adopts octahedral coordination geometry, with triphenylphosphine ligands occupying positions *trans* to the $Ru^I$-$Ru^I$ bond and carbonyl groups occupying *cis* positions at each $Ru^I$ center. A *trans*-staggered conformation is adopted about the $Ru^I$–$Ru^I$ bond, where *cis*-$Ru(CO)_2$ groups are rotated away from each other. The related tris(pyrazoyl)borate complex $[\{HB(pz)_3\}_2Ru_2(CO)_4]$ has a similar staggered $M_2L_{10}$ geometry, but with a *cis*-staggered conformation.[14]

Infrared and $^1H$ NMR spectroscopic data support a structure for $[(CH_3CN)_6Ru_2(CO)_4]^{2+}$ (**3**) similar to that of its triphenylphosphine derivative **4**, namely, a $C_2$-symmetric structure where the $PPh_3$ groups in **4** are replaced by $CH_3CN$ ligands, and either a *cis*-staggered or *trans*-staggered conformation is adopted, as in **a**.

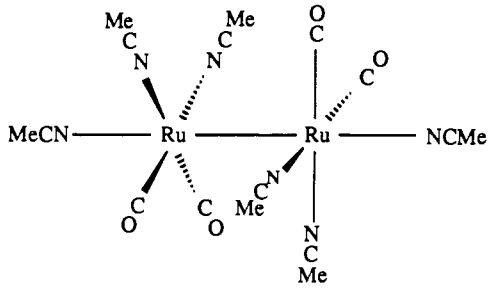


**a**

The infrared spectra of complexes **3** and **4** in Nujol mulls (see Figure 2) both display four carbonyl stretching vibrations in the terminal CO region, a pattern observed previously for both staggered[14] and eclipsed[10] $Ru_2(CO)_4^{2+}$ moieties in $L_6Ru^I_2(CO)_4$ complexes. The same pattern of four absorptions is also observed for **3** and **4** in $CH_3CN$ solution. The $^{13}C\{^1H\}$ NMR spectrum of complex **3** in $CD_2Cl_2$ solution at −80 °C displays two sets of $CH_3CN$ resonances and one CO resonance. Given that complex **3** in $CH_2Cl_2$ displays only terminal CO vibrations in its infrared spectrum, these observations are consistent with structure **a** for $[(CH_3CN)_6Ru_2(CO)_4]^{2+}$, assuming free rotation about the Ru–Ru bond on the NMR time scale.

**$[(Cp^*TiW_5O_{18})_2Ru_2(CO)_4]^{4-}$ (2).** Reaction of $[(CH_3CN)_6Ru_2(CO)_4](PF_6)_2$ with 2 equiv of $Cp^*TiW_5O_{18}(TBA)_3$ in $CH_2Cl_2$ solution yielded $[(Cp^*TiW_5O_{18})_2Ru_2(CO)_4](TBA)_4$, which could be isolated in 76% yield as analytically pure, light-sensitive material. Infrared spectroscopic data support a structure for **2** related to the structure of its $P_3O_9^{3-}$ analogue, **1**, by replacement of both $\kappa^3$-*O*-$P_3O_9^{3-}$ ligands (see Figure 1) with $\kappa^3$-*O*-$Cp^*TiW_5O_{18}^{3-}$ ligands. Unlike the $P_3O_9^{3-}$ ligand, $Cp^*TiW_5O_{18}^{3-}$ lacks a $C_3$ symmetry axis, with the result that different isomers can be generated for **2** in this fashion. The $C_{2h}$-symmetric isomer is shown in **b**.

The TBA salts of complexes **1** and **2** both display a single terminal CO stretching vibration and a single bridging CO stretching vibration in their IR spectra (see Figure 1), indicating a common *trans*-$Ru_2(\mu\text{-}CO)_2(CO)_2$ core structure. Infrared spectra of $[(Cp^*TiW_5O_{18})_2Ru_2(CO)_4](TBA)_4$ (Figure 4a), $[(Cp^*TiW_5O_{18})Ru(C_6H_6)](TBA)$[1] (Figure 4b), and $[(Cp^*TiW_5O_{18})Ir(1,5\text{-}C_8H_{12})](TBA)_2$[7a] (Figure 4c), recorded from Nujol mulls, are very similar in the 600–1000-$cm^{-1}$ metal–oxygen stretching region, supporting similar $\kappa^3$-*O*-$Cp^*TiW_5O_{18}^{3-}$ coordination for all three complexes as established X-ray crystallographically for the iridium complex.[7a]


**Figure 4.** Infrared spectra recorded from Nujol mulls of (a) $[(Cp^*TiW_5O_{18})_2Ru_2(CO)_4](TBA)_4$, (b) $[(Cp^*TiW_5O_{18})Ru(C_6H_6)](TBA)$, and (c) $[(Cp^*TiW_5O_{18})Ir(1,5\text{-}C_8H_{12})](TBA)_2$. Numerical data are given in the Experimental Section for spectrum a, ref 1 for spectrum b, and ref 7a for spectrum c.

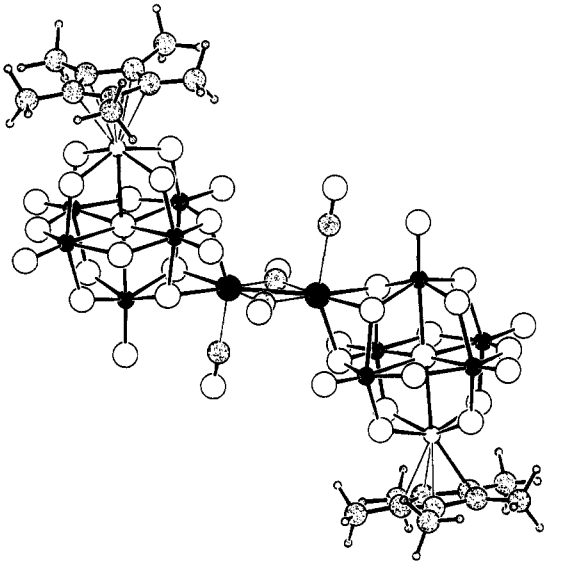

**b**

**$[(C_5H_5N)_6Ru_2(CO)_4]^{2+}$ (5) and $[(CH_3CO_2)_2(CH_3CN)_2Ru_2(CO)_4]$ (6).** As mentioned above, the $[(CH_3CN)_6Ru_2(CO)_4]^{2+}$ cation (**3**) is a very substitution-labile complex undoubtedly capable of serving as a precursor to numerous $L_6Ru^I_2(CO)_4$ complexes. It reacts with pyridine, for example, to form the hexasubstituted derivative $[(C_5H_5N)_6Ru_2(CO)_4]^{2+}$ (**5**). Complex **3** also reacts with bidentate ligands to form ligand-bridged derivatives such as the previously known acetate complex $[(CH_3CO_2)_2(CH_3CN)_2Ru_2(CO)_4]$.[14]

(14) Steyn, M. M. d. V.; Singleton, E.; Hietkamp, S.; Liles, D. C. *J. Chem. Soc., Dalton Trans.* **1990**, 2991.

## Experimental Section

**Reagents, Solvents, and General Procedures.** Unless stated otherwise, all operations were performed under an atmosphere of prepurified nitrogen or argon. The following were purchased from commercial sources and used without further purification: $[Ru(CO)_3Cl_2]_2$ (Strem), NaOH (Aldrich), $TlPF_6$ (Strem), $PPh_3$ (Aldrich), and pyridine (Mallinckrodt). The following solvents were distilled under nitrogen from the reagents indicated: $CH_3CN$ (Burdick and Jackson) from $CaH_2$, diethyl ether (anhydrous, Mallinckrodt) from Na/K alloy, methylene chloride (Fisher) from $P_4O_{10}$, and toluene (EM Science) and tetrahydrofuran (EM Science) from Na. Nitromethane (J. T. Baker) was dried over 3-Å molecular sieves (Linde Type A) that were activated by maintaining at 350 °C for 24 h and cooling to ambient temperature under vacuum. Literature procedures were followed to prepare $P_3O_9(TBA)_3{\cdot}2.5H_2O$[6b] and $Cp^*TiW_5O_{18}(TBA)_3$.[7b]

**Analytical Procedures.** Elemental analyses were performed by the School of Chemical Sciences Microanalytical Laboratory at the University of Illinois.

Infrared spectra were recorded from Nujol (mineral oil) mulls between KBr plates or from solutions in $CaF_2$ cells on a Nicolet 205 Fourier transform spectrometer. Absorptions are described as follows: strong (s), medium (m), weak (w), shoulder (sh), and broad (br).

$^1H$ and $^{13}C\{^1H\}$ NMR spectra were recorded either on a General Electric QE-300 or on a Varian XL-200 Fourier transform spectrometer and referenced internally to tetramethylsilane. $^{31}P$ NMR spectra were measured on a General Electric GN-300NB spectrometer. Chemical shifts were referenced externally to 85% aqueous $H_3PO_4$ using the sample replacement method. All NMR resonances are described as follows: singlet (s) and multiplet (m).

**Preparation of $[(P_3O_9)_2Ru_2(CO)_4](TBA)_4{\cdot}2H_2O$.** $[Ru(CO)_3Cl_2]_2$ (0.209 g, 0.408 mmol) was added in five portions to a solution of $P_3O_9(TBA)_3{\cdot}2.5H_2O$ (1.62 g, 1.60 mmol) in 10 mL of $CH_3CN$ over a 5-min period. The resulting deep orange solution was stirred at 25 °C for 3 h and then filtered to remove a trace amount of precipitate. Addition of diethyl ether (50 mL) caused an orange oil to separate which, after decanting the supernatant liquid, was converted to an oily precipitate by stirring twice with 50 mL of diethyl ether. After being dried for 10 min in vacuo, the solid was reprecipitated once from $CH_3CN$/diethyl ether (5 mL/40 mL) and once from $CH_2Cl_2$/diethyl ether (6 mL/10 mL). Final purification was achieved by cooling a $CH_2Cl_2$/ether (6 mL/5 mL) solution to −20 °C, isolating the large orange crystals which formed after a week by filtration at −20 °C, washing the crystals with 2 × 20 mL of diethyl ether, and drying them in vacuo. The yield was 0.33 g (0.184 mmol, 45% based on Ru). Anal. Calcd for $C_{68}H_{148}N_4Ru_2P_6O_{23}$: C, 45.53; H, 8.32; N, 3.12; Ru, 11.27; P, 10.36. Found: C, 45.52; H, 8.39; N, 3.34; Ru, 11.44; P, 10.54. IR (Nujol, 700–1325 $cm^{-1}$): 703 (s), 725 (sh), 737 (m), 771 (s), 798 (w), 845 (w), 880 (m), 891 (m), 947 (s), 1029 (w), 1063 (m), 1109 (sh), 1130 (s), 1276 (s), 1296 (s). IR (Nujol, 1650–2150 $cm^{-1}$; see Figure 2a): 1764 (s), 1951 (s) $cm^{-1}$. $^{31}P$ NMR (121.5 MHz, $CD_3CN$, 0.025 M, 20 °C): δ −9.87 (s). IR ($CH_3CN$, 0.01 M, 25 °C, 1650–2150 $cm^{-1}$): 1761 (s), 1924 (m), 1966 (s), 1980 (m). IR ($CH_3NO_2$, 0.007 M, 25 °C, 1650–2150 $cm^{-1}$): 1761 (m), 1925 (m), 1967 (s), 1982 (m).

**Preparation of $[(CH_3CN)_6Ru_2(CO)_4](PF_6)_2$.** A 0.944 M solution of NaOH in ethanol (2.07 mL, 1.95 mmol) was added dropwise over a 3-min period to a suspension of $[Ru(CO)_3Cl_2]_2$ (0.500 g, 0.975 mmol) in 30 mL of $CH_3CN$ with stirring. During the course of the addition, the solid $[Ru(CO)_3Cl_2]_2$ dissolved, yielding a cloudy, yellow solution. $TlPF_6$ (1.36 g, 3.9 mmol) was then added, with stirring, causing formation of a white precipitate in the yellow solution. The reaction mixture was then heated to reflux with stirring for 2.5 h, after which the white precipitate was removed by filtration and washed with 3 × 2 mL of $CH_3CN$. The deep-orange filtrate was next combined with the $CH_3CN$ washes, the volume was reduced to *ca.* 3 mL under reduced pressure, and 80 mL of diethyl ether was added to the concentrated solution with stirring to yield a deep-orange, oily precipitate. The supernatant was decanted off, and the residual paste was washed with 20 mL of diethyl ether and dried in vacuo for 30 min. The resulting crude product was then dissolved in 2.5 mL of $CH_2Cl_2$, leaving a small amount of white solid, which was removed by filtration. This solid was washed with 2 × 2 mL of $CH_2Cl_2$, and the washes were combined with the filtrate. Ether (65 mL) was added to this solution with stirring, generating an oily, orange precipitate. This precipitate was isolated by decanting the supernatant, washing with 2 × 15 mL of diethyl ether, and drying in vacuo for 30 min. It was then reprecipitated once more from 0.5 mL of $CH_3CN$/20 mL diethyl ether, isolated by filtration, and dried in vacuo for 10 min. Finally, sufficient $CH_3CN$ was added to the product to dissolve it, all volatiles were removed under reduced pressure, and the resulting material was dried in vacuo for 12 h, yielding 0.68 g (0.8 mmol, 82% yield based on Ru) of analytically pure, orange product. Anal. Calcd for $C_{16}H_{18}N_6O_4P_2F_{12}Ru_2$: C, 22.60; H, 2.13; N, 9.88; P, 7.28; Ru, 23.77. Found: C, 22.67; H, 2.15; N, 9.78; P, 7.15; Ru, 23.39. IR (Nujol, 1650–2150 $cm^{-1}$, see Figure 2c): 1970 (sh), 1989 (s, br), 2031 (s), 2062 (s) $cm^{-1}$. IR ($CH_3CN$, 0.006 M, 25 °C, 1650–2150 $cm^{-1}$): 1977 (br, sh), 1994 (s), 2033 (s), 2061 (m) $cm^{-1}$. IR ($CH_2Cl_2$, 0.012 M, 25 °C, 1650–2150 $cm^{-1}$): 1976 (br, sh), 1993 (s), 2033 (s), 2063 (m) $cm^{-1}$. $^{13}C\{^1H\}$ NMR (75.6 MHz, $CD_2Cl_2$ 0.25 M, −80 °C): δ 3.18 (s, *C*$H_3CN$), 3.28 (s, *C*$H_3CN$), 119.91 (s, $CH_3$*C*N), 125.33 (s, $CH_3$*C*N), 198.98 (s, *C*O).

**Reaction of $[(CH_3CN)_6Ru_2(CO)_4](PF_6)_2$ with Diethyl Ether.** A 0.47-g sample of $[(CH_3CN)_6Ru_2(CO)_4](PF_6)_2$ was stirred with 20 mL of diethyl ether at 25 °C for 10 min, and the supernatant was decanted. This washing procedure was repeated, and the solid obtained was dried in vacuo for 1 h. During the drying process, the color of the solid changed from yellow to green. About 10 mg of the green solid was put into a small test tube, which was then placed in a capped vial containing 0.2 mL of $CH_3CN$. The color of the solid in the tube changed back to yellow after about 1 h. This material was identified as $[(CH_3CN)_6Ru_2(CO)_4](PF_6)_2$ by elemental analysis (C, H, N). The remaining green solid was exposed to air for 12 h, and the color changed to yellow. The $^1H$ NMR of this yellow solid indicated the presence of about 0.013 mol of diethyl ether/mol of coordinated acetonitrile. Elemental analysis indicated that about 0.5 equiv of $CH_3CN$ had been replaced by diethyl ether per $Ru_2$ unit, most of which was removed in vacuo. Anal. Calcd for $C_{15.34}H_{18.09}N_{5.53}O_{4.47}F_{12}P_2Ru_2$ ($[(CH_3CN)_{5.53}(H_2O)_{0.4}(C_4H_{10}O)_{0.07}Ru_2(CO)_4](PF_6)_2$): C, 21.84; H, 2.16; N, 9.18; P, 7.34. Found: C, 21.94; H, 1.89; N, 9.08; P, 7.40.

**Preparation of $[(PPh_3)_2(CH_3CN)_4Ru_2(CO)_4](PF_6)_2$.** Reaction vessels were covered with aluminum foil throughout this preparation in order to minimize exposure to light. A solution of $[(CH_3CN)_6Ru_2(CO)_4](PF_6)_2$ (0.084 g, 0.099 mmol) in 2 mL of $CH_2Cl_2$ and a solution of $PPh_3$ (0.209 g, 0.797 mmol) in 3 mL of $CH_2Cl_2$ were mixed at 25 °C with stirring. A yellow precipitate appeared immediately. After 20 min of stirring, 13 mL of diethyl ether was added to increase the yield of precipitate. The precipitate was allowed to settle for *ca.* 2 h, isolated by filtration, washed with 3 × 10 mL of diethyl ether, and dried in vacuo for 2 h to yield 0.106 g of crude product. Analytically pure product (0.090 g, 0.070 mmol, 70% yield based on Ru) was obtained by cooling to −20 °C for 12 h a solution of crude product in 2 mL of $CH_3CN$ which was carefully layered over 7 mL of toluene, isolating by filtration the crystals obtained, washing them with 3 mL of toluene and with 3 mL of pentane, and drying them in vacuo for 12 h. Anal. Calcd for $C_{48}H_{42}F_{12}N_4O_4P_4Ru_2$: C, 44.59;

H, 3.27; N, 4.33; P, 9.58; Ru, 15.63. Found: C, 44.72; H, 3.31; N, 4.39; P, 9.39; Ru, 15.58. IR (Nujol, 600–1100 $cm^{-1}$): 645 (w), 695 (m), 704 (w), 746 (m), 759 (w), 841 (s, br), 860 (m), 880 (w), 999 (w), 1090 (m), 1097 (sh). IR (Nujol, 1650–2150 $cm^{-1}$; see Figure 2d): 1968 (m), 1983 (s), 2017 (s), 2040 (m). IR ($CH_3CN$, 0.006 M, 25 °C, 1650–2150 $cm^{-1}$): 1975 (sh), 1992 (s, br), 2026 (s), 2048 (m). $^{31}P\{^1H\}$ NMR (121.5 MHz, $CD_3CN$, 0.02 M, 25 °C): $\delta$ 22.4 (s).

**Preparation of $[(Cp^*TiW_5O_{18})_2Ru_2(CO)_4](TBA)_4$.** Reaction vessels were covered with aluminum foil throughout this preparation in order to minimize exposure to light. A mixture of $[(CH_3CN)_6Ru_2(CO)_4](PF_6)_2$ (0.105 g, 0.123 mmol) and $Cp^*TiW_5O_{18}(TBA)_3$ (0.538 g, 0.254 mmol) was dissolved in 4 mL of $CH_2Cl_2$. After standing at 25 °C for 30 min with stirring, the orange reaction solution was filtered, and the filtrate was combined with 2 × 1.5 mL of $CH_2Cl_2$ washes. A small amount of orange solid appeared in the filtrate due to solvent evaporation, and 50 mL of diethyl ether was added to complete the precipitation. After the light yellow supernatant was decanted, the orange, sticky residue was stirred with 3 × 12 mL of tetrahydrofuran until the wash became colorless. The resulting orange powder was then washed with 2 × 10 mL of diethyl ether and dried in vacuo at *ca.* 35 °C for 12 h. The yield was 0.391 g (0.0934 mmol, 76% yield based on Ru). Anal. Calcd for $C_{88}H_{174}N_4O_{40}Ru_2Ti_2W_{10}$: C, 26.00; H, 4.31; N, 1.38; Ru, 4.97; Ti, 2.36; W, 45.23. Found: C, 26.05; H, 4.40; N, 1.35; Ru, 4.88; Ti, 2.32; W, 45.33. IR (Nujol, 600-1000 $cm^{-1}$; see Figure 4a): 609 (w), 625 (w), 643 (sh), 654 (m), 722 (m), 739 (m), 773 (s), 795 (s), 835 (s, br), 882 (m), 957 (s), 970 (m), 981 (m). IR (Nujol, 1650-2150 $cm^{-1}$; see Figure 2b): 1808 (s), 1976 (s). $^1H$ NMR (200 MHz, $CD_3NO_2$, 25 °C): $\delta$ 2.09 (s, $C(CH_3)_5$).

**Preparation of $[(C_5H_5N)_6Ru_2(CO)_4](PF_6)_2 \cdot CH_2Cl_2$.** A solution of $[(CH_3CN)_6Ru_2(CO)_4](PF_6)_2$ (0.122 g, 0.143 mmol) in 3 mL of $CH_2Cl_2$ was added to a solution of pyridine (0.42 mL, 5.2 mmol) in 8 mL of $CH_2Cl_2$ with stirring at 25 °C. A yellow crystalline precipitate appeared, which was isolated by filtration, washed with 2 × 4 mL of $CH_2Cl_2$, and dried in vacuo for 1 h. The yield was 0.135 g (0.119 mmol, 83% based on Ru). Anal. Calcd for $C_{35}H_{32}N_6Cl_2F_{12}O_4P_2Ru_2$: C, 36.13, H, 2.77; N, 7.22; P, 5.32; Ru, 17.37. Found: C, 36.29; H, 2.73; N, 7.25; P, 5.48; Ru, 17.19. IR (Nujol, 600–2150 $cm^{-1}$): 609 (w), 629 (w), 684 (sh), 699 (m), 710 (m), 733 (m), 762 (m), 843 (s), 884 (m), 897 (sh), 960 (w, br), 1011 (w), 1020 (w), 1044 (w), 1070 (w, br), 1156 (w), 1166 (w), 1217 (w), 1227 (w), 1279 (w), 1302 (w, br), 1490 (w), 1604 (m), 1610 (sh), 1720 (w, sh), 1743 (s), 2001 (s), 2013 (m). $^1H$ NMR (200 MHz, $CD_3NO_2$, 25 °C): $\delta$ 5.46 (s, $CH_2Cl_2$), 7.62 (t, br, $NC_5H_5$), 8.11 (t, br, $NC_5H_5$), 8.61 (d, br, $NC_5H_5$).

**Preparation of $[(CH_3CO_2)_2(CH_3CN)_2Ru_2(CO)_4]$.** A mixture of $[(CH_3CN)_6Ru_2(CO)_4](PF_6)_2$ (0.040 g, 0.047 mmol) and $CH_3COONa \cdot 3H_2O$ (0.128 g, 0.84 mmol) was ground to a fine powder and stirred in 4 mL of $CH_2Cl_2$ at 40 °C for 5 h. A yellow precipitate formed during this period. Diethyl ether (8 mL) was then added, generating more yellow precipitate. After 30 min of stirring, the supernatant was removed by filtration. The solid obtained was then dried in vacuo at 80 °C for 20 min, washed twice with 2 mL of $CH_2Cl_2$, and dried in vacuo at 25 °C for 10 min. This material was added to 2 mL of $CH_3CN$, and the mixture was heated to 80 °C with stirring for 20 min. The residual insoluble colorless powder was removed by filtration and washed with 1 mL of $CH_3CN$. The filtrate was combined with the $CH_3CN$ wash and concentrated to *ca.* 0.3 mL. About 4 mL of diethyl ether was then added with stirring, and the solution was allowed to stand at −15 °C for 12 h, yielding yellow crystals. These crystals were collected by filtration, washed with 2 mL of diethyl ether, and dried in air at 25 °C for 1 h. The yield was 19 mg (0.037 mmol, 78% based on Ru). The IR spectrum of the product in $CHCl_3$ solution was identical to the one reported for authentic material in ref 10a.

**Reaction of $[(CH_3CN)_6Ru_2(CO)_4](PF_6)_2$ with $P_3O_9(TBA)_3$.** A solution of $[(CH_3CN)_6Ru_2(CO)_4](PF_6)_2$ (0.030 g, 0.035 mmol) in 1 mL of $CH_2Cl_2$ was added dropwise over a 2-min period to a solution of $P_3O_9(TBA)_3 \cdot 2.5H_2O$ (0.094 g, 0.093 mmol) in 1 mL of $CH_2Cl_2$ with stirring, yielding an orange solution. The solvent was removed in vacuo, and the resulting orange solid was dissolved in $CD_3CN$. The $^{31}P$ NMR spectrum (121.5 MHz, 20 °C) of this solution showed that $[(P_3O_9)_2Ru_2(CO)_4](TBA)_4$ ($\delta$ −9.87) was produced in 90% yield.

**X-ray Crystal Structure Determinations[12] of $[(P_3O_9)_2Ru_2(CO)_4](TBA)_4 \cdot 2CH_3CN$ (I) and $[(PPh_3)_2(CH_3CN)_4Ru_2(CO)_4](PF_6)_2$ (II).** Single crystals of I were grown from $CH_3CN$/diethyl ether at −20 °C. A yellow crystal of dimensions 0.2 × 0.3 × 0.3 mm was used for data collection. The 0.2 × 0.2 × 0.3 mm yellow crystal of II used for data collection was grown by layering a $CH_3CN$ solution of II on top of toluene and allowing the solvents to interdiffuse.

Details of the crystal structure determination[12] of I (II) are summarized in Table I. Data having $2\theta$(Mo K$\alpha$) < 46° (50°) were collected at −75 °C (20 °C) on an Enraf-Nonius CAD4 automated K-axis diffractometer (Syntex $P2_1$ automated four-circle diffractometer). From a total of 7180 (3920) measured independent reflections, 4615 (2924) with $I > 2.53\sigma(I)$ were taken as "observed" and used for all calculations. The structure was solved by "direct methods", SHELXS-86 ("heavy-atom" Patterson methods, SHELXS-86), and difference Fourier syntheses. In the final cycle of least-squares refinement, anisotropic thermal coefficients were refined for all non-hydrogen atoms. The final agreement factors were $R$[11] = 0.039 and $R_w$[11] = 0.043 ($R$ = 0.043 and $R_w$ = 0.050).

Fractional atomic coordinates and relevant bond lengths and angles for the anion of I and cation of II are given with estimated standard deviations in Tables II–V. Final atomic coordinates, anisotropic thermal parameters for non-hydrogen atoms, and complete sets of bond lengths and angles involving non-hydrogen atoms in I and II are given with estimated standard deviations in Tables SI–SVI.[12] Perspective drawings are also provided for the anion of I (Figure 1), the cation and solvent molecule of I (Figure S1[12]), and the cation of II (Figure 3).

**Acknowledgment.** We thank the National Science Foundation for financial support. Dr. Scott Wilson of the University of Illinois School of Chemical Sciences X-ray Crystallographic Laboratory performed the X-ray crystal structure determinations.

**Supplementary Material Available:** Crystal structure analysis reports and tables of atomic coordinates, thermal parameters, bond lengths, and bond angles for $[(P_3O_9)_2Ru_2(CO)_4](TBA)_4 \cdot 2CH_3CN$ and $[(PPh_3)_2(CH_3CN)_4Ru_2(CO)_4](PF_6)_2$ and perspective plots of the $TBA^+$ anion and $CH_3CN$ solvent molecule of the former compound (27 pages). Ordering information is given on any current masthead page.